LM-00K052
June 30, 2000

# New Measurements of the Solubility of Metal Oxides at High Temperature

G.A. Palmer, P. Benezeth, D.J. Wesolowski, S.A. Wood, C. Xiao

## NOTICE

# New Measurements of the Solubility of Metal Oxides at High Temperatures

D. A. Palmer, P. Bénézeth, D. J. Wesolowski, S. A. Wood*, and C. Xiao
Chemical and Analytical Sciences Division, Oak Ridge National Laboratory
Building 4500S, P.O. Box 2008, Oak Ridge, Tennessee 37831-6110, U.S.A.
* visiting scientist, Department of Geology, University of Idaho, Moscow ID 83844, U.S.A.

The results of high temperature solubility studies at ORNL are presented in which mainly direct pH measurements were made of aqueous solutions in contact with the crystalline solid phases: $Al(OH)_3$, AlOOH, $Fe_3O_4$, $Mg(OH)_2$, $Nd(OH)_3$, and ZnO. Examples are highlighted of specific phenomena such as: the kinetics of gibbsite and boehmite dissolution and precipitation; the appearance of metastable equilibria in the dissolution of $Fe_3O_4$; the extremely rapid precipitation of crystalline brucite, $Mg(OH)_2$; and anomalies in the apparent solubility profiles of AlO(OH) and ZnO. General trends associated with the effects of temperature and ionic strength are mentioned. Some of the potentiometric investigations were augmented by conventional batch {AlO(OH) and ZnO}, and flow-through column {ZnO} experiments. In the additional case of $ZnCr_2O_4$, the extremely low solubility of this spinel permitted application of only the latter technique and these results are discussed in terms of the measured chromium levels that resulted from incongruent dissolution.

## 1. Introduction

Knowledge of the solubility of metal oxides and hydroxides in aqueous solutions under controlled conditions is of direct value in understanding natural and industrial processes, as well as yielding the thermodynamics of the metal-containing species in solution that are in equilibrium with these solid phases. Indeed, owing to the high degree of insolubility of most oxides in near neutral pH solutions, solubility measurements usually provide the only means of identifying and quantifying these dissolved species. During the last decade, measurements have been carried out at ORNL on the oxides/hydroxides of $Al(OH)_3$ [1-3], AlOOH [4,5], $Fe_3O_4$, $Mg(OH)_2$ [6], $Nd(OH)_3$ [7], ZnO [8,9], and $ZnCr_2O_4$ up to 300°C. Although some of these solid phases have been studied quite extensively in the past, our new measurements take advantage of recent advances in analytical techniques, the application of *in situ* pH monitoring, and experience with flow-through methods, (e.g., [10]), or combinations of these.

The hydrogen-electrode concentration cell (HECC) was pioneered at ORNL for use in measuring the pH of homogeneous aqueous solutions to its upper working limit of 300°C. These studies included measurements of dissociation constants of weak acids and bases, and the hydrolysis and complexation of metal ions. However, the cell was also found to provide stable potential readings of metal oxide/hydroxide suspensions in aqueous electrolytes [4]. Moreover, the changes in pH with time associated with dissolution or precipitation following the isothermal addition of acid or base, can be interpreted in terms of the rates of these processes, while also allowing the equilibrium solubility to be determined from both under- and supersaturation [11]. Obviously pH is a critical variable in acidic and basic regions where the pH dependence of $\log[\Sigma m(M(OH)_n^{v-n}]$ {v = valence of M} is $\geq$ |3,2, or 1|. At intermediate conditions, the metal concentrations are generally too low to allow pH to be calculated accurately from mass balance considerations and non-complexing, thermally-stable pH buffers are scarce to non-existent.

A brief description of the use (and limitations) of the HECC in studies of metal oxide/hydroxide (MO) solubilities is given here. The operating range of this cell is 0 to 300°C. The cell consists of two compartments separated by a liquid junction with the following compositions in a typical experiment with an acidic reference:

reference: $H_2$,Pt | HX($m_1$),NaX($m_2$)
test: $H_2$,Pt | HX($m_1$) or NaOH($m_3$),NaX($m_4$),$MO_{cr}$

In order to minimize activity coefficient differences and liquid junction potentials, ratios of $m_1$:$m_2$; and $m_1$ or $m_3$:$m_4$ were <0.1; in other words, a supporting, non-complexing, strong electrolytic medium (NaX) is required for this cell to function. The hydrogen ion concentration in the test compartment ($pH_m$ is defined as $-\log[H^+]$) is determined relative to the known concentration in the reference compartment from the Nernst equation:

$$\log[H^+] = \log m_{H^+ ref} - F(E+E_{LJ})/(2.3026RT) \quad (1)$$

where E is the measured cell potential, $E_{LJ}$ is the estimated liquid junction calculated from the complete Henderson equation [12], and F, R, and T represent the Faraday constant, the universal gas constant and the temperature in Kelvin, respectively.

**2. Aluminum Solubility: AlOOH and $Al(OH)_3$**

The most comprehensive solubility study conducted to date at ORNL with the HECC involved measurements with boehmite {AlOOH} from 100 to 290°C in NaCl solutions (0.03 to 5 molal) over a wide range of $pH_m$, supported by conventional batch experiments. The solubility equilibria that needed to be considered pertained only to mononuclear species as summarized in Eq. 2.

$$AlOOH_{cr} + (3\text{-}n)H^+ = Al(OH)_n^{3-n} + (2\text{-}n)H_2O \quad (2)$$

These equilibria are represented by the general equation for the solubility quotients ($Q_{sn}$: n = 0-4):

$$Q_{sn} = [Al(OH)_n^{3-n}]/[H^+]^{3-n} \quad (3)$$

Multiple titrations were performed beginning at high and low $pH_m$ at virtually every condition. This established the reproducibility of the method and the integrity of the reference solution over the time period of a titration (generally up to one month with solution samples being withdrawn twice daily). Moreover, by adding either acidic or basic titrant, the equilibrium solubility can be approached from over- or under-saturation, thereby verifying the attainment of equilibrium. Typically, each data set, comprising the results of multiple titrations carried out at each temperature and ionic strength, was treated by least-squares regression based on Eq. 3. Complementary data were obtained at 0.03, 1.0 and 5.0 molal ionic strength from solubility measurements made with conventional batch experiments at relatively high acid and base concentrations where the free acid or base could be calculated unambiguously from mass balance. Under these conditions, direct $pH_m$ measurements are unnecessary and ambiguous due to high liquid junction potentials and difficulty maintaining excess supporting electrolyte. However, as the $pH_m$ range was found to be very narrow, over which the $Al(OH)^{2+}$ and $Al(OH)_2^+$ species were prevalent, the value for $Q_{s1}$ was taken from independent, homogeneous titration data [13] for the hydrolysis equilibrium,

$$Al^{3+} + H_2O = Al(OH)^{2+} + H^+ \quad (4)$$

and the value of $Q_{s0}$ (Eq. 3). Figure 1 shows a typical solubility profile resulting from six independent titrations with comparisons to the previously-published batch experiments [14,15], extrapolated from the corresponding $Q_{sn}$ values reported at infinite dilution.

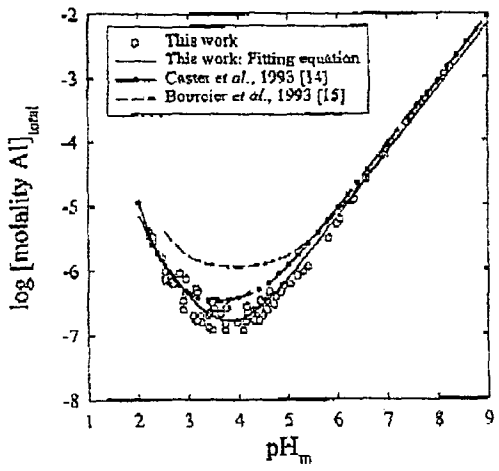


Figure 1. Solubility profile for boehmite at 203.3°C in 0.03m ionic strength (NaCl).

The agreement between our results and those of previous investigators is consistently good on the base side where the aluminate anion predominates, solubilities are high, and $pH_m$ can be calculated from the excess free base. However, at intermediate $pH_m$ values near the solubility minimum, where $Al(OH)_3^0$ is the primary aqueous aluminum specie, our results are consistently lower, although quite similar to those of Castet *et al.* [14] at lower temperatures. This is a manifestation of the advantage of direct $pH_m$ measurement obviating the need for $pH_m$ buffers that potentially complex metal ions and possibly adsorb to the oxide surfaces, thereby changing the stoichiometry of the buffer mixture. Independent measurements of complexation can be made, but this introduces further experimental uncertainty. Finally, in the current experiments, equilibrium was always approached from supersaturation at the solubility minima and hence the observation of lower solubilities cannot be due to inadequate equilibration times.

As pointed out above, effective operation of the HECC requires the presence of excess salt in solution, which is advantageous in studying the effect of ionic strength on the solubility quotients. These effects are inherently greatest for highly charged ions such as $Al^{3+}$. The stability of $Al^{3+}$ is enhanced with increasing ionic strength, whereas that of $Al(OH)_4^-$ is raised to a lesser extent, resulting in a much narrower solubility profile than shown in

Figure 1, for example. In other words, the intermediate hydrolysis species become even less important, and in fact the solubility of boehmite can be modeled effectively with only knowledge of the quotients, $Q_{s0}$, $Q_{s1}$, and $Q_{s4}$. This reduces the number of experiments that need to be made and eliminates the difficult analytical problem of determining ppb levels of aluminum in the presence of high salt concentrations.

The solubility quotients, $Q_{s0}$ and $Q_{s4}$ were calculated from the results of an extensive series of batch equilibrations involving gibbsite {$Al(OH)_3$}, covering conditions from 6 to 80°C at ionic strengths to 5 molal. These values were used to constrain the fits of the corresponding quotients determined from the higher temperature boehmite experiments, using the standard Gibbs energies of the two solid phases. Thus a complete thermodynamic description of the $Al^{3+}$ and $Al(OH)_4^-$ ions is available from ambient to 300°C and high ionic strengths.

The equilibration times are generally found to be much shorter in the HECC than in typical batch reactors, generally requiring less than eight hours to reach equilibrium following an isothermal addition of titrant. Thus, the kinetics of dissolution or precipitation can be monitored via the $pH_m$ reading in real time following an addition of base or acid, either in a near-to or far-from equilibrium mode. In fact, the dissolution and precipitation rates of boehmite were too fast to observe large changes (i.e., far-from equilibrium), so that the utility of this method is demonstrated better with gibbsite at lower temperatures as illustrated in Figure 2. First, note that the solubility curve was derived from a series of batch experiments [3] with buffered solutions, which took about two years to complete at this one condition, and similar equilibrations in acidic [2] and basic solutions [3] (*cf.*, the titrations shown in Figure 1 each took an average of 20 days to complete). Second, the agreement between the batch results and the equilibrium values obtained with the HECC is obviously excellent. Third, Figure 2 shows the $pH_m$ changes associated with each addition of acidic titrant that can be interpreted quantitatively in terms of the kinetics of precipitation of gibbsite. Solution samples were withdrawn after each equilibration to establish each new equilibrium value.

As should be the case in all solubility studies, the solid phases, gibbsite and boehmite, were characterized in detail for assurance that no phase change had occurred, or metastable surface layers had been formed, or that no physical degradation of the solid particles had taken place.

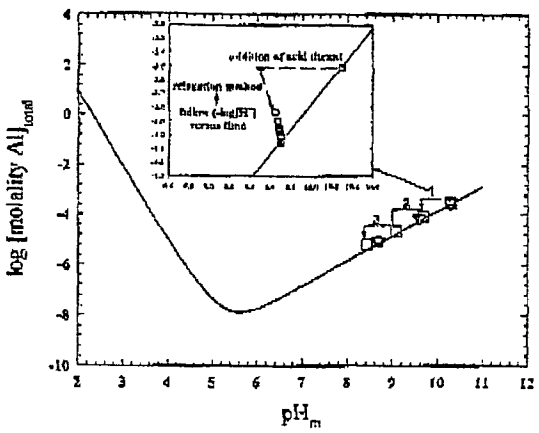


Figure 2. Solubility profile for gibbsite at 50°C in 0.1 molal ionic strength, NaCl, from batch experiments [3] showing the paths of repetitive additions of acidic titrant in the HECC.

### 3. Iron Solubility: $Fe_3O_4$

Magnetite is the principal corrosion product of steel in high temperature industrial environments under all but the most oxidizing conditions, where hematite, $\alpha$-$Fe_2O_3$, becomes stable. Therefore, detailed information on the solubility of magnetite is essential in modeling the transport of iron in hydrothermal solutions and in the hydrothermal alteration of iron-bearing materials. $Fe^{2+}$ and its hydrolysis products, $Fe(OH)_y^{2-y}$, are the dominant aqueous iron species over a wide range of Eh-pH conditions. However, due to the low solubility of iron oxides in near-neutral and basic solutions, homogeneous speciation studies of aqueous iron have proven difficult. Current models for the speciation of ferrous iron are based mainly on experimental studies of magnetite solubility [16-18], which are highly discrepant at basic pH's. The more recent experimental literature results [16,17] predict much lower magnetite solubilities in neutral to basic solutions than the earlier study [18].

The solubility of Alfa *AESAR* magnetite was measured as a function of $pH_m$ at 150, 200 and 250°C in 0.1 molal sodium trifluoromethane-sulfonate, NaTr. The same technique was employed as described above for the aluminum system. At the hydrogen partial pressures used in this study, 15-20 bars, Fe(III) aqueous species are insignificant, and the total iron in solution at a given $pH_m$ is determined by the reactions

$$1/3Fe_3O_{4\,cr} + 2H^+ + 1/3H_{2,g} = Fe^{2+} + 4/3H_2O \qquad (5)$$

$$Fe^{2+} + yH_2O = Fe(OH)_y^{2-y} + yH^+ \qquad (6)$$

where y ranges from 1 to 3. An acidic reference solution was used to obviate the problem of slow decomposition of NaTr in alkaline solutions. The measured total iron in the test solutions at low $pH_m$ were more than an order of magnitude below the predicted levels [16-18], despite the fact that all three previous studies are in excellent agreement in the acidic $pH_m$ range, where $Fe^{2+}$ is the dominant iron solution species. Similar results were obtained at 200°C. In order to investigate further this phenomenon, a second pump was employed, so that the titrations from basic to acidic conditions, in which equilibrium is approached from undersaturation, could be "reversed" using a basic titrant. It was found that the observed solubility followed the predicted stoichiometry of reaction (5). Furthermore, the forward titration values generally fell well below the reverse titration values, apparently bracketing an equilibrium state, which is slow in achieving final equilibrium.

Early in this experimental program, a series of experiments was conducted with the same acidic reference solutions, but with a strongly acidic test solution, consisting of 0.01 molal HTr in NaTr (I=0.1 molal), at temperatures of 150, 200 and 250°C. In all cases, magnetite was partially or completely converted to well-crystallized hematite, as evidenced by the red color and XRD patterns of the run products. The $pH_m$ of the experimental solutions was also observed to drift upward, finally stabilizing after 36-60 hours at 150°C and after 6-8 hours at 250°C. The final $pH_m$ values and the ratio of hematite/magnetite in the final product correlated directly with the initial solution acidity and mass of solid. In other words, only 0.1-0.2 grams of magnetite were used, so the extent of conversion of magnetite to hematite observed was consistent with the amount of $H^+$ consumed during the reaction, and the measured iron contents in solution varied linearly with the inverse square of the $H^+$ concentration. These observations are consistent with the redox-disequilibrium, incongruent dissolution of magnetite via the reaction:

$$Fe_3O_{4\,cr} + 2H^+ \rightleftharpoons Fe_2O_{3\,cr} + Fe^{2+} \qquad (7)$$

Note that the hydrogen fugacity or partial pressure at which magnetite and hematite are in redox equilibrium at these temperatures is many orders of magnitude lower than the 15-20 bars employed in our experiments.

Reaction (7) appears to be reversible, despite the instability of hematite at these hydrogen fugacities. This may be an acid-catalyzed metastable reaction, since our results in more basic solutions are consistent with the redox equilibrium dissolution and precipitation of magnetite according to reactions (5,6). It is important to note that the solubility of magnetite according to reaction (7) is independent of hydrogen fugacity, while that of reaction (5) decreases with the 1/3 power of the hydrogen fugacity. Thus, at lower hydrogen partial pressures, as were employed in the previous magnetite solubility studies [16,18], the iron levels in solution predicted from these two reactions would approach one another. However, hematite was not reported in the post-experiment solid phase in any of these previous studies, although it was reported [16,17] that an additional phase was formed in the upstream section of their columns, which were interpreted from XPS analyses to be $Fe(OH)_2$. Perhaps the high liquid/solid ratios in our study, coupled with the much lower solubility of the redox disequilibrium assemblage, promoted the formation of hematite in our experiments. Alternatively, the presence of about 15% hematite in our starting material may have catalyzed the reversibility of the redox disequilibrium reaction, although sufficient hydrogen overpressure was imposed to quantitatively convert the hematite to magnetite.

**4. Magnesium Solubility: $Mg(OH)_2$**

In the natural environment, brucite, $Mg(OH)_2(s)$, is formed principally from the serpentinization process, where local ground waters in the vicinity may have pH values in excess of 11, and the species $Mg(OH)^+$ is one of the dominant magnesium(II) aqueous species. Magnesium hydrolysis is also important in industrial processes such as desalinization and the production of magnesium from sea water. The hydrolysis of $Mg^{2+}$ to form $Mg(OH)^+$ was studied in our laboratories using the HECC to 250°C [19]. However, during the initial stages of this investigation an abrupt $pH_m$ buffering effect was observed after ca. 4% hydrolysis. Upon opening the HECC, a precipitate was observed and an XRD analysis revealed it to be crystalline brucite. Therefore, a complementary study [6] of brucite precipitation was carried out at 60°, 100°, 150°, and 200°C in 0.10 and 1.0 mol $kg^{-1}$ (NaCl) from a homogeneous solution that provided very precise data for the equilibrium,

$$Mg(OH)_{2\,cr} \rightleftharpoons Mg^{2+} + 2H^+ \qquad (8)$$

which was achieved within minutes of the addition of basic titrant to the test compartment of the HECC. This example is merely given here to indicate another mode of operation of this technique for specific cases.

**5. Neodymium solubility: $Nd(OH)_3$**

Solubility studies of crystalline $Nd(OH)_3$ were completed recently in our laboratory using a HECC to 290°C and ionic strengths of 1 molal (NaTr). The solubility in acidic solution, where $Nd^{3+}$ dominates the speciation, decreases with increasing temperature reflecting the general observation that $Q_{s0}$ is an inverse function of temperature. The extrapolated, infinite dilution $K_{s0}$ values proved to be in fair agreement (±0.5 log units compared with the experimental uncertainty at 25°C of ±0.3 log units) with some previous low temperature results, but much larger variations were also found. It is suggested that in some previous work the solid phase was contaminated with surface layers of less soluble $Nd(OH)CO_3$. Thus, the current study has provided an empirical equation that yields $Q_{s0}$ values as a function of temperature to 300°C and ionic strength to 1 molal. Differentiation with respect to temperature provided a reliable enthalpy of dissolution of $Nd(OH)_3$ due to the wide temperature range investigated. The $\Delta H_f^\circ$ value for $Nd(OH)_{3\,cr}$ derived therefrom (-1414 ± 5 kJ·mol$^{-1}$) is in excellent agreement with the value reported by Merli *et al.* [20] of -1415.5 ± 1.4 kJ·mol$^{-1}$.

The solubility quotients of the intermediate hydrolyzed species, $Nd(OH)_2^+$ and $Nd(OH)^{2+}$, were determined only at 250 and 290°C where they become more important at low $pH_m$, but still are dominant only over a narrow $pH_m$ range as was observed for the aluminum analogues. It was found that estimates [21] of $K_{s1}$ were two orders of magnitude higher than measured in this study. Similarly, the solubility minimum defined by the $Nd(OH)_3^0$ specie is about three orders of magnitude lower than previously estimated [21].

**6. Zinc Solubility: ZnO**

The solubility of zincite has been studied extensively using the HECC technique with excellent reversibility and reproducibility being demonstrated in acidic [8] and basic [9] solutions. Under these conditions, equilibrium was attained very rapidly and $Zn^{2+}$ and $Zn(OH)_3^-$, respectively were shown to be the dominant dissolved zinc species. In the former case, excellent agreement with the model of Ziemniak [22] was achieved and independent experiments in 0.03m NaOH using stirred batch reactors and flow-through methods to 300°C confirmed the latter assignment. However, at temperatures >200°C in near neutral $pH_m$ solutions where $Zn(OH)_2^0$ dominates the speciation in solution, difficulties arose that could have been due to the formation of a hydrated layer on the ZnO surfaces. The scattered results obtained at these conditions were rejected in favor of a model that involved extrapolation of $Q_{s2}$ values obtained at lower temperature (≤200°C) for $Zn(OH)_2^0$ formation. More recent flow-cell work, in which acid was injected into the stream as it exited the cell inside the furnace, indicates that precipitation during sampling may have been the cause of scattered and generally lower solubilities reported in our HECC work [9]. Indeed, these new data are in agreement with the highest solubilities reported earlier [9], suggesting that precipitation in the sampling line was an irregular event. Note, that similar problems occurred initially in our boehmite solubility experiments over a narrow $pH_m$ range on the basic side of the solubility minima. However, these were overcome by placing a platinum frit at the entrance to the sampling line, thus preventing seed crystals of boehmite from entering the line.

**7. Zinc Chromite Solubility: $ZnCr_2O_4$**

This final example is presented for a number of reasons. First, attempts to study the solubility of this spinel failed using both the HECC and standard batch techniques. In the main, the failures were due to the exceedingly low solubility of $ZnCr_2O_4$, for which Cr(III) levels in solution were on the order of 10ppt (parts per trillion). This meant that large solution samples were needed and this is not practical even in one-liter capacity pressure vessels [4]. Second, contamination is a major problem with limited volume systems where the solid phase and plumbing systems must be thoroughly flushed before representative samples can be obtained. Third, the equilibration rates appeared to be slow, and this is not practical for the HECC due to concerns of being unable to maintain the integrity of the reference solution over long periods of time. Fourth, the required presence of excess supporting electrolyte introduces possible low-level metal ion impurities and analytical matrix interferences. Fifth, there was an initial concern that the hydrogen atmosphere in the HECC could reduce the Cr(III) in solution. Therefore, these experiments were carried out in a titanium flow-through column with inert platinum and PEEK™ plumbing.

A detailed description of this work is beyond the scope of this presentation, but it is useful to consider some salient features of the techniques employed and the chemistry behind the dissolution of zinc chromite. The chromium concentrations that should have exceeded those of zinc by a factor of two if indeed $ZnCr_2O_4$ dissolved in a "normal" congruent fashion were found to be considerably lower than the equivalent zinc concentration. This indicated that this spinel dissolved in an incongruent manner. This conclusion was supported by the later observation of a decrease in the Zn/Cr ratio by *ca.*

6% in the solid material recovered from the upstream end of the column. Note that the amount of zinc preferentially leached from the column was minor compared to the amount of solid in the column so that the supply of zinc was not depleted, which is another potential disadvantage of the batch or HECC technique in this case. Moreover, the concentrations of chromium approached those for CrOOH and $FeCr_2O_4$ measured independently by Ziemniak *et al.* [23]. Therefore, the zinc concentration was controlled by the equilibrium,

$$ZnCr_2O_{4\,cr} + 2H^+ \rightleftharpoons 2CrOOH_{cr} + Zn^{2+} \qquad (9)$$

with appropriate considerations of the hydrolysis of $Zn^{2+}$ at high pH [9], whereas the total chromium concentration was defined by the equilibria,

$$CrOOH_{cr} + H_2O \rightleftharpoons Cr(OH)_3^0 \qquad (10)$$

$$Cr(OH)_3^0 + H_2O \rightleftharpoons Cr(OH)_4^- + H^+ \qquad (11)$$

at the relatively high $pH_m$ values employed in this study (i.e., dilute $NH_3$ and NaOH solutions). This incongruent dissolution behavior is similar to the metastable leaching of ferrous iron from magnetite described by equation (7), where the concentration of ferric ions was below the detection limits of the GFAA (graphite-furnace atomic absorption) method.

Clearly these are difficult measurements and great care is needed to avoid contamination, while the availability of sensitive analytical methods, such as ICPMS (inductively-coupled plasma mass spectrometry) and chemiluminescence, is mandatory if reliable and meaningful thermodynamic data are to be extracted.

**Conclusion**

A number of representative two-phase {aqueous – solid metal oxide/hydroxide} systems have been presented with the aim of indicating the advantages and current limitations of carrying our solubility experiments in stirred hydrogen-electrode concentration cells. General and specific facets of the chemistry involved in these studies have also been highlighted. The use of either other electrodes that do not require reducing hydrogen gas, or a HECC in flow-through mode [24] may further expand the utility of this approach.

**References**

[1] D.J. Wesolowski, Geochim. Cosmochim. Acta, 56, 1065 (1992).
[2] D.A. Palmer, D.J. Wesolowski, Geochim. Cosmochim. Acta, 56, 1093 (1992).
[3] D.J. Wesolowski, D.A. Palmer, Geochim. Cosmochim. Acta. 58, 2947 (1994).
[4] D.A. Palmer, P. Bénézeth, D.J. Wesolowski, Geochim. Cosmochim Acta, submitted.
[5] P. Bénézeth, D.A. Palmer, D.J. Wesolowski, Geochim. Cosmochim Acta, submitted.
[6] P.L. Brown, S.E. Drummond, D.A. Palmer, J. Chem. Soc., Dalton Trans., 3071 (1996).
[7] S.A. Wood, D.A. Palmer, D.J. Wesolowski, P. Bénézeth, Geochem. Soc., in press.
[8] D.J. Wesolowski, P. Bénézeth, D.A. Palmer, Geochim. Cosmochim. Acta, 62, 971 (1998).
[9] P. Bénézeth, D.A. Palmer, D.J. Wesolowski, Geochim. Cosmochim. Acta, 63, 1571 (1999).
[10] S.E. Ziemniak, M.E. Jones, K.E.S. Combs, J. Sol. Chem., 21, 1153 (1992).
[11] P. Bénézeth, D.A. Palmer, D.J. Wesolowski, Proc. World Geothermal Congress, Japan, (2000).
[12] C.F. Baes, Jr., R.E. Mesmer, *The Hydrolysis of Cations*, John Wiley and Sons, New York, 489p. (1976).
[13] D.A. Palmer, D.J. Wesolowski, Geochim. Cosmochim. Acta, 57, 2929 (1993).
[14] S. Castet, J.L. Dandurand, J. Schott, R. Gout, Geochim. Cosmochim. Acta, 57, 4869 (1993).
[15] W.L. Bourcier, K.G. Knauss, K.J. Jackson, Geochim. Cosmochim. Acta, 57, 747 (1993)
[16] P.R. Tremaine, J.C. LeBlanc, J. Sol. Chem., 9, 415 (1980).
[17] S.E. Ziemniak, M.E. Jones, K.E.S. Combs, J. Sol. Chem., 24, 837, (1995).
[18] F.H. Sweeton, C.F. Baes, Jr., J. Chem. Therm., 2, 479 (1970).
[19] D.A. Palmer, D.J. Wesolowski, J. Sol. Chem., 26, 217 (1997).
[20] L. Merli, B. Lambert, J. Fuger, J. Nucl. Chem., 247, 172 (1997).
[21] J.R. Hass, E.L. Shock, D.C. Sassini, Geochim. Cosmochim. Acta, 59, 4329 (1995).
[22] S.E. Ziemniak, J. Sol. Chem., 21, 745 (1992).
[23] S.E. Ziemniak, M.E. Jones, K.E.S. Combs, J. Sol. Chem., 27, 33 (1998).
[24] F.H. Sweeton, R.E. Mesmer, C.F. Baes, Jr., J Physics E, 6, 165 (1973).

This research was sponsored by EPRI, Inc. under the direction of project manager, Dr. P. Frattini, and by the Division of Chemical Sciences, Geosciences, and Biosciences, Office of Basic Energy Sciences, U.S. Department of Energy, under contract DE-AC05-00OR22725 with Oak Ridge National Laboratory, managed and operated by UT-Battelle, LLC.